Electronic Supplementary Material (ESI) for Lab on a Chip.

Laser Printing-Enabled Direct Creation of Cellular Heterogeneity in Lab-on-a-Chip Devices

Ruitong Xiong, Wenxuan Chai, Yong Huang

Supplementary Information

SI1. CFD simulation with designed channel

CFD simulation was implemented using ANSYS FLUENT R16.0 (ANSYS, Canonsburg, PA), and the 3D model with tetrahedron meshes are shown in Fig. S1(A). To simulate the flow field in the designed channel, the viscosity of the fluid was set as 0.94 cP based on the property of typical cell culture medium[1]. Since the average flow rate was 2.5 mL/min, the boundary conditions were set with a mass flow rate of 4.2×10^{-5} kg/s at the inlet and 0 gauge pressure at the outlet, and the wall condition was set as no slip. To analyze whether the flow in the designed chip is laminar, the Reynolds number ($\mathrm{Re}=\frac{\rho u L}{\mu}$, where ρ is the density of the fluid, u is the velocity of the fluid with respect to the object, L is the characteristic linear dimension and μ is the dynamic viscosity of the fluid) in each computational cell within the model was calculated as shown in Fig. S1(B). Since the Reynolds number is much smaller than 2300, it is confirmed that the flow in the designed channel is laminar. The total pressure distribution on the bottom of the upper channel is illustrated in Fig. S1(C), and the total pressure value along the central line of the bottom of the upper channel is shown in Fig. S1(D). It can be seen from Fig. S1(C) and (D) that with the proposed design and flow rate, the total pressure on the bottom of the upper channel has no significant difference along the flow direction.

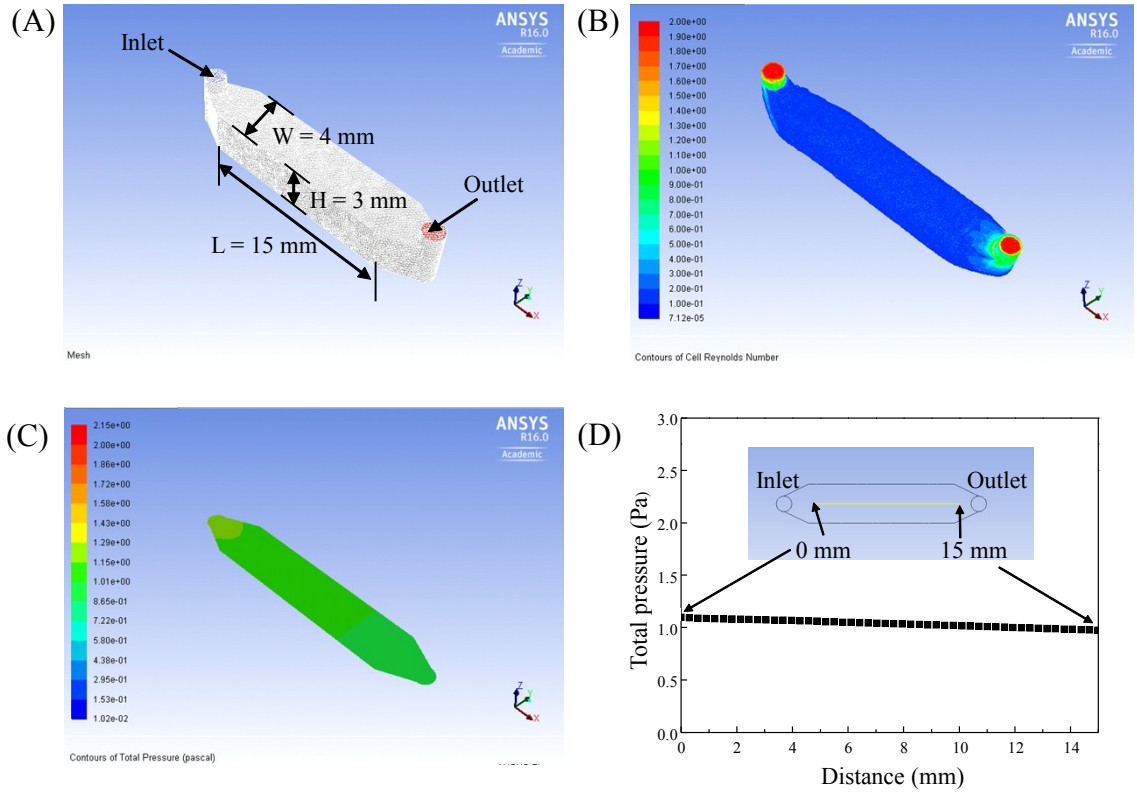

Fig. S1. (A) 3D meshes for CFD simulation. (B) Contour of Reynold numbers in all the cells of the simulation model. (C) Contour of total pressure distribution on the bottom of the upper channel. (D) Total pressure distribution along the central line of the bottom of the upper channel.

SI2. Fabrication PDMS components by PEGDA-based mold casting

The PEGDA mold was fabricated from the designed shape using a digital micromirror device (DMD)-based stereolithography (SLA) system, which was customized by integrating a digital light processing (DLP)-based projector (Infocus, Portland, OR), a motorized vertical stage (Thorlab, Newton, NJ) and other related accessories. The whole SLA system, set up as a bottom-up configuration, is shown in Fig. S2(A). Before printing, pure PEGDA precursor (M_n 700, Sigma-Aldrich, St. Louis, MO) was mixed with 0.50% (w/v) photo-initiator diphenyl(2,4,6-trimethylbenzoyl)phosphine oxide (Sigma-Aldrich, St. Louis, MO) and 1% UV-absorbing Glominex Pigment (Coolglow, Carrollton, TX). After the PEGDA structures were printed on an aluminum printing substrate which was sprayed with a thin layer of black paint, as shown in Fig. S2(B), the printing substrate was covered with a plastic piece with a 40 × 20 × 3 mm cavity, exposing the printed PEGDA structures, to create PEGDA-based lower and upper molds for casting. Then mixed silicone elastomer base and curing agent (Sylgard® 184, Dow Corning, Auburn, MI) at a weight ratio of 10:1 were poured into the molds as shown in Fig. S2(C). Once cured, the gelled PDMS lower and upper components were peeled off from the molds.

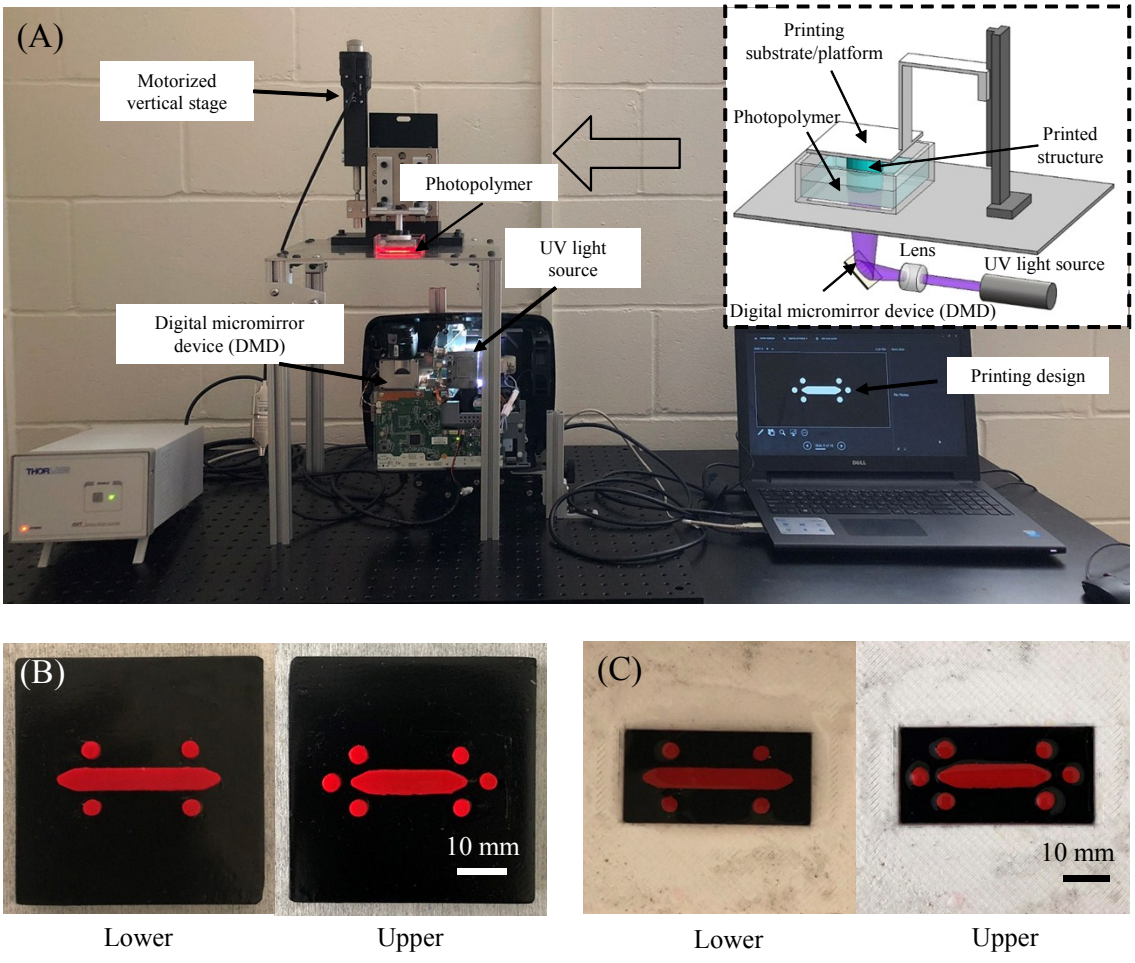

Fig. S2. (A) Customized stereolithography system (inset: working mechanism schematic), (B) printed PEGDA structures on the printing substrate, and (C) assembled PEGDA molds for PDMS casting.

SI3. Lab-on-a-chip system integration

The assembled chip with the laser-printed patterns was connected with a Masterflex L/S peristaltic pump (Cole-Parmer, Vernon Hills, IL) by tubes and connectors from both the inlet and outlet of the upper channel to introduce a pulsatile flow into the chip. All the required parts to integrate the whole lab-on-a-chip system are listed in Table S1. Before the integration, all the required parts in the system were sterilized by autoclaving, and all the assembly and integration work was performed in a biosafety hood to avoid possible contamination. In order to filter the air entering into the cell culture medium reservoir (1395 laboratory storage bottle), 15 mm diameter filter with 0.2 μm pore was mounted in the GL45 3-hole delivery cap. The L/S 14 silicon tubing was clamped in the pump head to roll with it and drive the circulation of the supplied cell culture medium. The C-flex tubing was used to connect everything together with luer locks and adapters. The set plugs were used to plug the inlet and outlet of the lower channel during incubation. After the chip was incubated 48 hours, the cell culture medium in the lower channel was refreshed through these two ports. For parallel evaluation of cellular behavior using fibroblasts, 40 mL of Dulbecco's Modified Eagle's Medium (DMEM, Sigma-Aldrich, St. Louis, MO) supplemented with 10% fetal bovine serum (FBS; HyClone, Logan, UT) and 1% antibiotic-antimycotic solution was filled into the cell culture medium reservoir to be perfused through the system. For targeted drug delivery for MCF-7 breast cancer cells, 40 mL of Minimum Essential Medium (MEM, Sigma-Aldrich, St. Louis, MO) supplemented with 10% fetal bovine serum (FBS; HyClone, Logan, UT), 5 μg/mL insulin and 1% antibiotic-antimycotic solution was supplied to the system for perfusion.

Table S1. List of parts for lab-on-a-chip system integration

Part name	Amount*	Company
Pump drive (Masterflex L/S variable-speed economy drive)	1	Cole-Parmer
Pump head (Masterflex Easy-Load pump head)	2	Cole-Parmer
Silicon tubing (L/S 14)	2	Cole-Parmer
C-flex clear tubing (1/8" OD)	4	Cole-Parmer
Male luer with lock ring with 1/16" hose barb	12	Cole-Parmer
Female luer-female luer adapter	8	Cole-Parmer
Corning® GL45 3-hole delivery cap	1	Corning
Corning® 15 mm diameter filters, 0.2 μm pore	1	Corning
Corning® 1395 laboratory storage bottle	1	Corning
LuerTight set plug	2	Kinesis

*For tubing, the number indicates the amount of segments.

SI4. Laser printing apparatus and printing process observation

Laser printing was implemented as laser-induced forward transfer in this study. The system mainly consisted of a beam delivery system and a 193 nm, 12 ns full-width half-maximum argon fluoride excimer laser (Coherent ExciStar, Santa Clara, CA) with a laser spot size of 150 μm in diameter. The materials to be printed were coated with 50 μm thickness on the back side of an ultraviolet (UV) quartz support (85% transmittance for 193 nm laser; Edmund Optics, Barrington, NJ) pre-coated with a layer of gelatin energy absorbing layer with 10 μm thickness to form a ribbon for printing as used before[2]. The applied laser fluence was measured by a FieldMax laser power/energy meter (Coherent, Santa Clara, CA). The laser pulse frequency was set to be 10 Hz as previously reported[2]. Linear motorized *xy* stages (Thorlabs, Newton, NJ) were utilized to drive the linear movement of the ribbon for continuous exposure of new coating material to be printed. The movement of the receiving substrate was controlled using a set of *xyz* translational stages (Aerotech, Pittsburg, PA). The direct-writing height was set to be 2 mm during the laser printing process.

The jet formation and impingement process of bioinks printed under different laser fluences were observed and compared to identify the applicable laser fluence to print each bioink. The jet formation and impingement process was recorded with a JetXpert imaging system (ImageXpert Inc., Nashua, NH) based on a time-resolved imaging approach. After each laser pulse, a trigger signal was sent from the laser system to the imaging system to capture a frame of the formed jet at certain delay time. Under a certain printing condition, a series of images were captured using different delay times of different jets and complied together to represent the jet formation and impingement process. The applicable laser fluence to print a certain bioink was identified based on the observed droplet/jet formation process and impingement types by following the criteria as discussed in a previous study[3]. Based on the observed results, laser fluence (after considering a 85% transmittance of the quartz support) of 600 mJ/cm^2 was chosen for printing of the bioink consisted of 1.00% NaAlg, 3.00 mg/mL collagen and 2.5×10^6 cells/mL fibroblasts. In particular, laser fluence of 500 mJ/cm^2 was chosen for printing the bioink consisted of 0.50% NaAlg, 3.00 mg/mL collagen and 2.5×10^6 cells/mL fibroblasts, and the representative images of the jet formation and impingement process under this condition is shown in Fig. S3(A). Laser fluence of 350 mJ/cm^2 was chosen for printing of the bioink consisted of 0.25% NaAlg, 3.00 mg/mL collagen and 2.5×10^6 cells/mL fibroblasts, and the representative images of the jet formation and impingement process under this condition is illustrated in Fig. S3(B). Laser fluence of 300 mJ/cm^2 was chosen for printing of the bioink consisted of 3.00 mg/mL collagen and 2.5×10^6 cells/mL fibroblasts, and the representative images of the jet formation and impingement process under this condition is presented in Fig. S3(C).

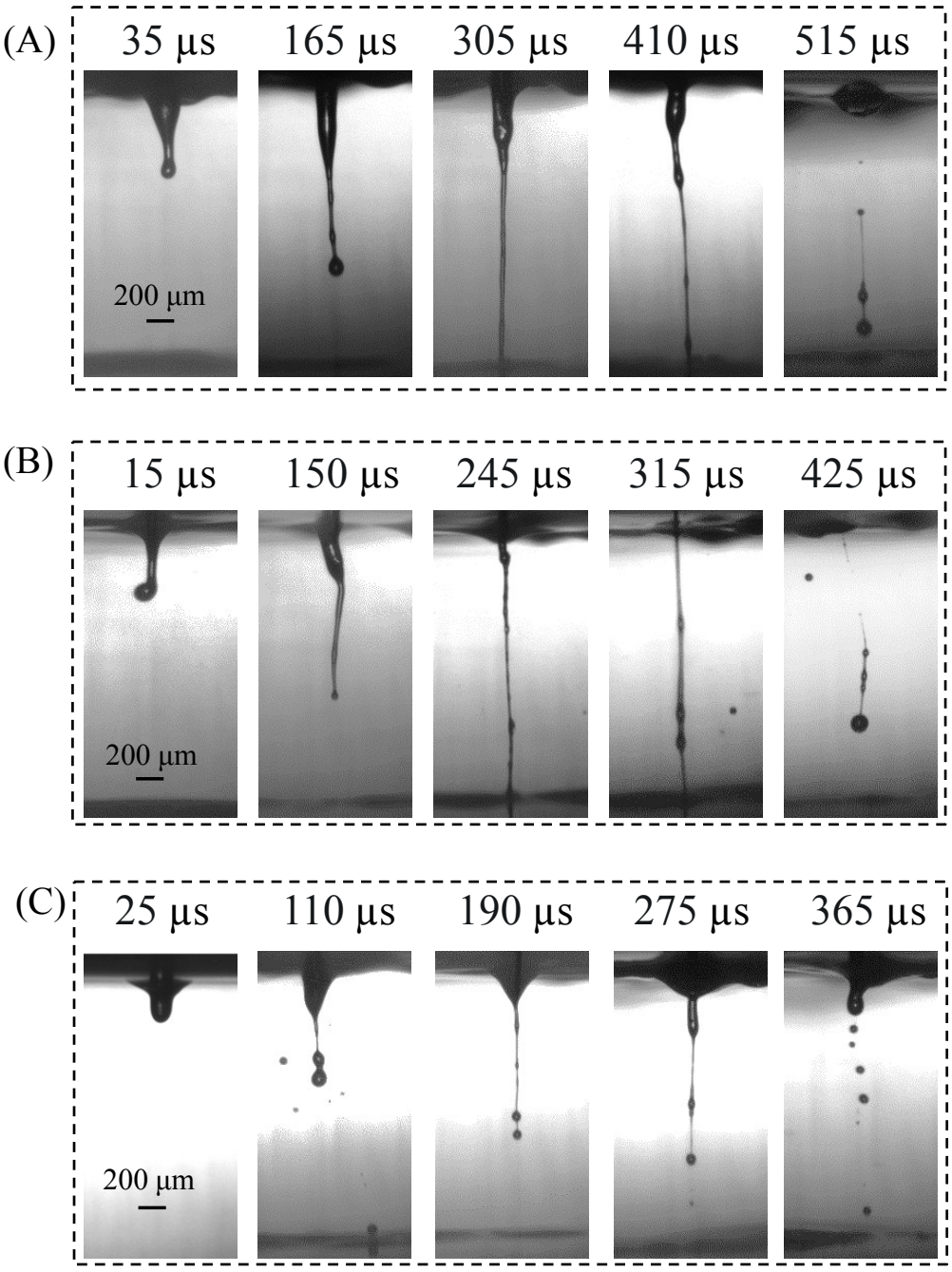

Fig. S3. (A) Images of jet formation and impingement process during printing 0.50% alginate with 3.00 mg/mL collagen and 2.5×10^6 cells/mL fibroblasts at 500 mJ/cm^2. (B) Images of jet formation and impingement process during printing 0.25% alginate with 3.00 mg/mL collagen and 2.5×10^6 cells/mL fibroblasts at 350 mJ/cm^2. (C) Images of jet formation and impingement process during printing 3.00 mg/mL collagen and 2.5×10^6 cells/mL fibroblasts at 300 mJ/cm^2.

SI5. Cell viability immediately after printing

Immediately after printing, the viability of cells in printed cellular patterns for cellular behavior evaluation was measured. Each pattern was carefully transferred into a centrifuge tube containing 100 μL of 0.055 mol/L sodium citrate (VWR, West Chester, PA) to dissolve the cross-linked alginate in the gel for 10 minutes (skip this step for the patterns without alginate). Then it was transferred into another centrifuge tube containing 100 μL 0.50% (w/v) collagenase (Sigma-Aldrich, St. Louis, MO) solution to dissolve the cross-linked collagen in the gel at 37℃ for another 10 minutes. Then each suspension with dissociated cells was centrifuged at 1000 rpm for 5 min to remove the supernatant. The pellet in the centrifuge tube was then mixed with 10 μL of 0.4% trypan blue (Sigma-Aldrich, St. Louis, MO) solution to stain the cells. The stained cells were observed under an optical microscope (EVOS XL, Grand Island, NY) with a hemocytometer to determine the cell viability. The cell viability of the four cellular patterns immediately after printing is shown in Fig. S4.

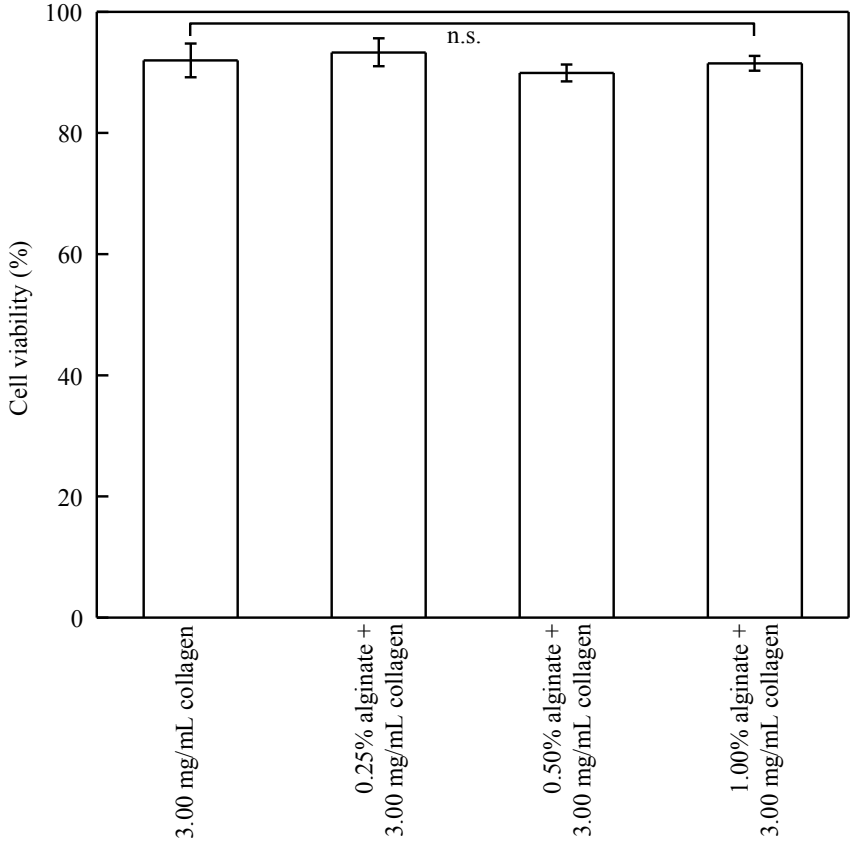

Fig. S4. Cell viability of the four cellular patterns immediately after printing. Difference between each group is not statistically significant (n.s.; error bar indicates ± one standard deviation, $p < 0.05$, $n = 3$).

SI6. Rheological characterization of ECM gel properties

Before each collagen and alginate ECM gel was characterized for its frequency dependent storage modulus (G'), a strain sweep was firstly performed in shear strain from 0.01% to 1% at a frequency of 1 Hz to confirm the linearly elastic regime. The characterized storage modulus as a function of shear strain of each gel is shown in Fig. S5. It is confirmed that gels at a shear strain of 0.50% are in the linearly elastic regime. Therefore, the shear strain of 0.50% was utilized during the frequency sweep.

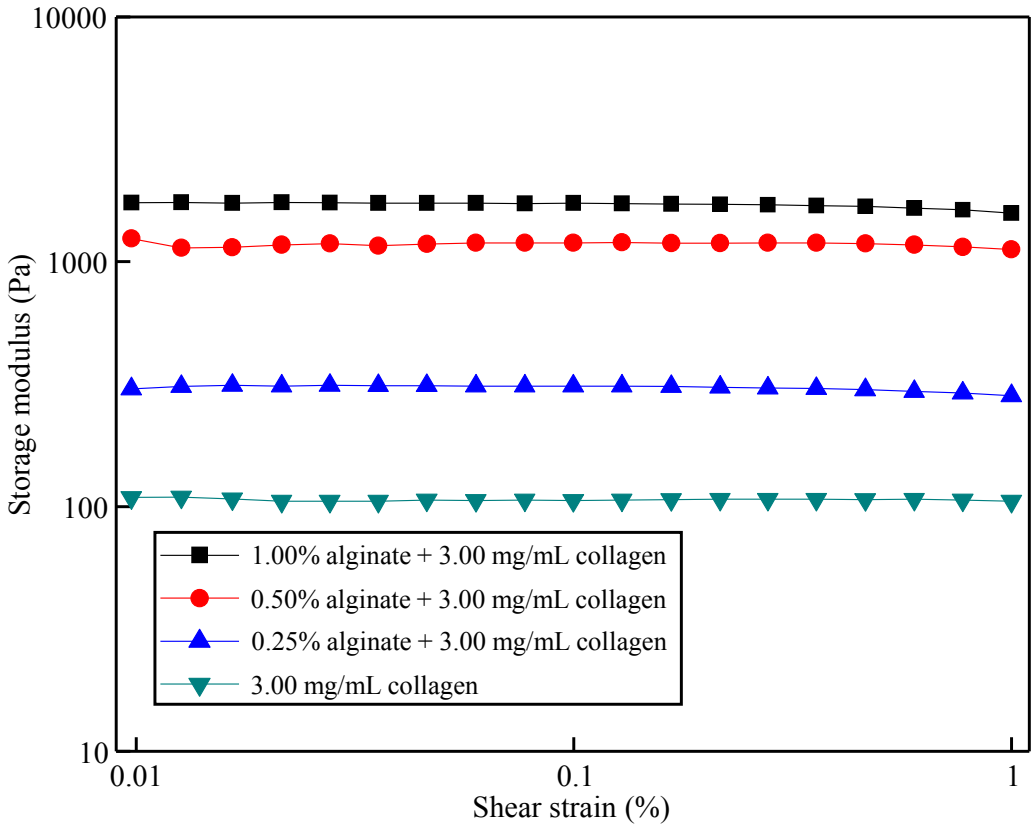

Fig. S5. Storage modulus as a function of shear strain at 0.01% to 1%.

SI7. Measurement of ECM diffusion coefficient

The amount of FITC-dextran (70 kDa, Sigma-Aldrich, St. Louis, MO) released from each pattern/gel after a certain time (M(t)) and infinite time (M(∞)) was determined based on the fluorescence intensity of supernatant containing FITC-dextran collected in the experiments. The ratio between M(t) and M(∞)is shown in Fig. S6 as a function of time for each gel. Based on the results shown in Fig. S6, the diffusion coefficient of each gel was calculated.

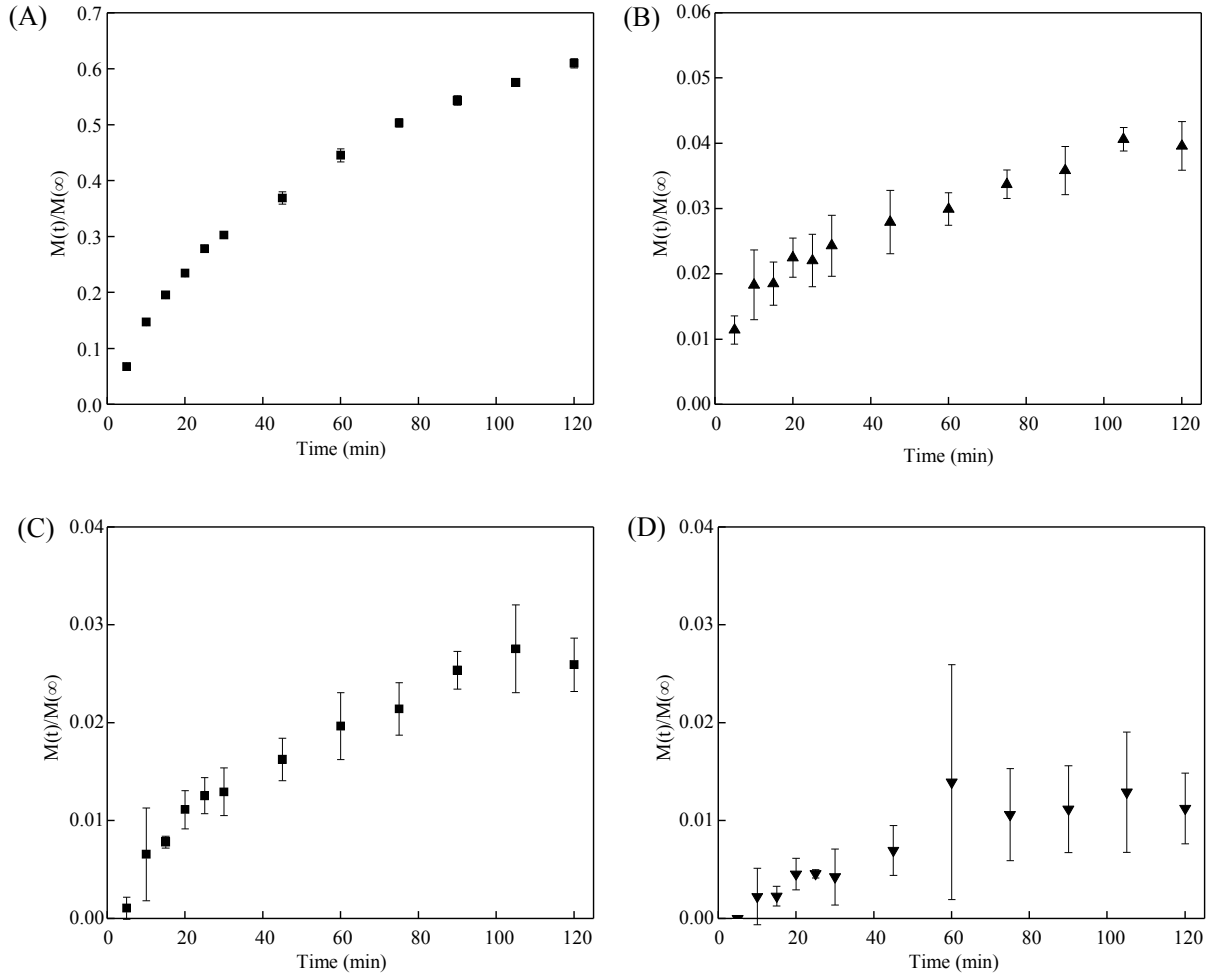

Fig. S6. Ratio of M(t)/M(∞) as a function of time for (A) 3.00 mg/mL collagen, (B) 0.25% alginate and 3.00 mg/mL collagen, (C) 0.50% alginate and 3.00 mg/mL collagen, and (D) 1.00% alginate and 3.00 mg/mL collagen.

SI8. Comparisons of cell patterning methods

The comparisons of three typical cell patterning methods, which are photolithography, contact printing (also called stamping[4]) and microfluidic patterning, with the LIFT-based printing method are listed in Table S2 in terms of the material compatibility, geometric feasibility and process complexity.

Table S2. Comparisons of cell patterning methods

	Typical cell patterning methods			
	Photolithography	Contact printing/ stamping	Microfluidic patterning	LIFT-based printing
Material compatibility	• Often not directly applicable to proteins and cells[9] • Cell adhesion materials required[10]	• Substrate requires a higher affinity towards the ink than the stamp[7] • Difficult to create patterns with three or more materials[6, 7]	• Material should be able to flow when driven by capillary forces, pressure or electro-osmosis effect[11]	• Material should have good printability • No limitations on the variety of materials to be deposited
Geometric feasibility	• 2D patterns easily created with computer-aided design (CAD)[7] • Less feasible in creating multi-layered structures	• Less feasible in creating multi-layered structures • Size of stamp should be fitted into designed channels	• Pattern geometries are limited to open network structures[8]	• 2D patterns easily created following CAD[12] • Able to create multi-layered and 3D structures
Process complexity	• Require additional cell seeding • Clean-room facility required[4]	• Required pre-created master with photolithography[5]	• Required pre-created channels or chambers	• Laser printing system required • Direct creation of cellular patterns

References

1. E. Fröhlich, G. Bonstingl, A. Höfler, C. Meindl, G. Leitinger, T. R. Pieber and E. Roblegg, *Toxicol. In Vitro*, 2013, 27, 409-417.
2. R. Xiong, Z. Zhang, W. Chai, D. B. Chrisey, and Y. Huang, *Biofabrication*, 2017, 9, 024103.
3. Z. Zhang, R. Xiong, D. T. Corr and Y. Huang, *Langmuir*, 2016, 32, 3004-3014.
4. A. Folch and M. Toner, *Annu. Rev. Biomed. Eng.*, 2000, 2, 227-256.
5. L. Filipponi, P. Livingston, O. Kašpar, V. Tokárová, and D. V. Nicolau, *Biomed Microdevices*, 2016, 18, 9.
6. J. Tien, C. M. Nelson, and C. S. Chen, *Proc. Natl. Acad. Sci.*, 2002, 99, 1758-1762.
7. D. Falconnet, G. Csucs, H. M. Grandin, and M. Textor, *Biomaterials*, 2006, 27, 3044-3063.
8. E. Delamarche, A. Bernard, H. Schmid, A. Bietsch, B. Michel, and H. Biebuyck, *J Am. Chem. Soc.*, 1998, 120, 500-508.
9. G. M. Whitesides, E. Ostuni, S. Takayama, X. Jiang, D. E. Ingber, *Annu. Rev. Biomed. Eng*., 2001, 3, 335-373.
10. T. H. Park and M. L. Shuler, *Biotechnol. Prog*., 2003, 19, 243-253.
11. G. S. Fiorini, and D. T. Chiu, *BioTechniques*, 2005, 38, 429-446.
12. S. V. Murphy, and A. Atala, *Nature Biotechnol*, 2014, 32, 773.